

On the dynamics of semiflexible fibrin gels

M. De Spirito^{†*}, G. Arcovito[†], F. Andreasi Bassi[†] and F. Ferri^{††}.

[†] *Istituto di Fisica, and INFM, Facoltà di Medicina e Chirurgia, Università Cattolica del Sacro Cuore, L.go F. Vito, 1 - 00168-Roma, Italy*

^{††} *Dipartimento di Scienze Chimiche, Fisiche e Matematiche and INFM, Università dell'Insubria, sede di Como, Via Lucini 3, I-22100 Como, Italy*

SUMMARY: The internal dynamics of semiflexible fibrin gels has been investigated by means of dynamic light scattering (DLS). Fibrin gels, grown at room temperature from fibrinogen solutions at different NaCl concentrations, exhibit rather different structural features. High salt concentrations produce “fine” gels characterized by thin fibers and small mesh sizes, while low salt concentrations give rise to “coarse” gels with thick fibers and much larger mesh sizes. The observed dynamics of these two kinds of gels are quite different as well. “Fine” gels behave as typical semiflexible polymer gels, in which the dynamic structure factor $f(q,t)$ shows an initial monoexponential decay followed by a stretched exponential decay, $f(q,t) \sim \exp(-(\Gamma_q t)^\beta)$. Conversely, “coarse” gels exhibit a highly arrested dynamics, in which the dynamic structure factor does not relax to zero, but decays to a plateau whose value depends on the scattering wavevector q . Moreover, only the stretched exponential decay is observed at the fastest decay times, with the exponent $\beta = 0.63 \pm 0.07$ being independently of q . This behaviour can be interpreted as given by the contributions of the internal elastic modes of many different length scales.

*E-mail of the corresponding author: despirito@caspur.it

Introduction

A gel represents a unique state of matter characterized by space-filled ramified structures responsible for the macroscopic solid-like properties of the sample. Depending on the mechanical properties of the constituent elements of the gel and on the mechanism of the gelation process, one may obtain gels with quite different structural and elastic characteristics.

Polymer gels are three-dimensional networks of entangled polymer chains whose stiffness is responsible for many of the gel properties. While the dynamics of polymer gels formed by rigid rods or random coils is fairly well understood²⁾, for the networks formed by polymers with a stiffness intermediate between the above two limiting cases, the so called semiflexible polymers, there are still controversial theories²⁾.

Biopolymer gels, and in particular fibrin gels, offer the opportunity to address this issue because they are classical example of gels obtained from semiflexible polymers^{2,3)} whose properties have been intensively studied over the last half century. Fibrin gels are the basic structural element of the blood cloth playing a key role in blood coagulation processes and in many other emorheology problems⁴⁾. The knowledge of the physical properties of the fibrin gel is of fundamental importance to understand its role in many physio-pathological processes, and it is known⁴⁻⁶⁾ that these properties are determined, to a large extent, by the physical properties of the fibrin fibers, such as their diameter, elastic modulus, resistance to proteolysis, etc. Fibrin gels are formed by fibrin polymers grown from solutions of fibrinogen macromolecules activated by some specific enzyme. Fibrinogen is a centro-symmetric high molecular weight plasma glycoprotein (MW ~ 340,000), rod-like in shape, ~47 nm in length and ~6 nm thick, that consists of a central globular domain joined by two extended connectors to two outer globular domains⁴⁻⁶⁾. When the fibrinogen interacts with some specific enzyme, such as thrombin in the case of vertebrates, it becomes a reactive protein called monomeric fibrin. This happens because the enzyme removes two couples of small peptides from the central domain, uncovering two pairs of polymerization sites, *A* and *B*, which are complementary to two sites (*a* and *b*) always present on the two outer domains. The site *A* is uncovered first, and this activation leads to a slightly peculiar polymerization mechanism⁴⁾ where the monomers first proceed to form two-stranded, half-staggered protofibrils. Only successively, when the *B* site is uncovered, the protofibrils aggregate with each other to form branched fibers bundles, which eventually branch, yielding a three-dimensional gel.

The gel structure can be controlled, by changing the physical-chemical parameters of the gelling solution such as salt concentration, ionic strength, pH values, and can be continuously changed between two limiting classes in which fibrin gels are customarily classified⁴⁾: “coarse” and “fine” gels. “Coarse” gels are large-pore gels made up of thick fibers while “fine” gels are narrow-pore gels made up of thin fibers. Much experimental work has been performed since the early 50's on the fibrin gel structure, mainly using electron microscopy

techniques, demonstrating the importance of fibrin fibers diameter in determining the physical properties of the fibrin gel⁴⁻⁶⁾. Recent static light scattering studies⁷⁾ carried out on coarse gels, showed that the gel fibers are entangled together according to an almost linear self-similar structure characterized by a mass fractal dimension $D_m \sim 1.2$. For these gels, the typical mesh sizes range from a few to tens of microns, while the average diameters of the fibers are around 100 nanometers.

In this paper, dynamic light scattering (DLS) data on both “fine” and “coarse” fibrin gels are presented. Our preliminary results show that “fine” and “coarse” gels exhibit completely different dynamics, which can be explained by taking into account the very different mechanical properties of the two types of gels.

Materials and Methods

Purified solutions of human fibrinogen (Calbiochem, San Diego, CA, USA (Cat. #341576, lot B10707)) were diluted in the appropriate buffer (50 mM TRIS-HCl, 0.001 M EDTA, pH 7.4) to reach the desired final fibrinogen (~ 0.1 mg/ml) and NaCl (0.1 or 0.5 M) concentration. The final fibrinogen solution was filtered through a $0.22 \mu\text{m}$ pore low retention filter (Millex-GS, Millipore, Milano, Italy) directly in a carefully cleaned scattering cell. To start the reaction, human thrombin (Sigma-Aldrich, Milano, Italy (Cat. #T-6759, lot 104H9314)) was added under rapid stirring to the fibrinogen solution to a final molar ratio of 1:100.

To perform DLS measurements we used an ALV/SLS-5000 system from ALV, Langen, Germany, equipped with a 4 W Argon laser (Innova 70, Coherent, FRG) operating at 800 mW at 488 nm. The detection of the scattered light was carried out with a mono-mode fiber coupled to a photomultiplier, both mounted on a stepping motor-controlled rotating arm. The autocorrelation function was performed using a digital, 256 logarithmic scaled channels, correlator (ALV5000). The sample, contained in a cylindrical cell (8 mm inner diameter) immersed in a toluene-filled index-matching vat, could be rotated during the measuring time and its temperature controlled to $25 \pm 0.1^\circ\text{C}$. With this specific set-up we have access to a range of the scattering angle θ in between 25 and 150, corresponding to a range of wavevectors q between 3.0×10^4 and $3.3 \times 10^5 \text{ cm}^{-1}$ ¹⁻⁴⁾, being $q = 4\pi n/\lambda \sin(\theta/2)$,

where λ is the vacuum wavelength of the light and n is the refractive index of the medium. A more detailed description of this instrument can be found in Refs. (3,7).

The dynamic light scattering technique⁸⁾ is based on the determination of the normalized time-averaged intensity autocorrelation function

$$g_T^{(2)}(q, t) = \frac{\langle I(q, 0) I(q, t) \rangle_T}{\langle I(q) \rangle_T^2} \quad (1)$$

where $I(q, t)$ is the intensity of the light scattered from a sample at the delay time t and at the angle θ , corresponding to a wavevector q , and T is the integration time. In order to describe the material properties responsible of the dynamic behaviour, we need to extract, from the autocorrelation function, the normalized ensemble-averaged dynamic structure factor

$$f(q, t) = \frac{\langle E(q, 0) E^*(q, t) \rangle_E}{\langle I(q) \rangle_E} \quad (2)$$

where $E(q, t)$ is the scattered electric field at delay time t and $\langle \dots \rangle_E$ denotes ensemble average. The relation between $g_T^{(2)}(q, t)$ and $f(q, t)$ depends on the particular sample being studied. Typically, i.e. for ergodic samples, the well-known Siegert relation⁸⁾ applies, and it results that

$$f(q, t) = \sqrt{g_T^{(2)}(q, t) - 1} \quad (3)$$

Conversely when the ensemble average could not be replaced by the temporal average, i.e. for non ergodic samples such as gels or dense solutions, $g_T^{(2)}(q, t)$ depends on the specific spatial configuration probed in the experiment, and Eq. 3 does not hold. Several attempts have been made to overcome such strong limitation in the investigation of complex systems, since P. Pusey and Van Megen suggested a model independent approach⁹⁾. According to their theory, $f(q, t)$ can still be recovered from a single sample configuration, provided that ensemble-averaged scattered intensity $\langle I(q) \rangle_E$ is known. This is given by⁹⁾

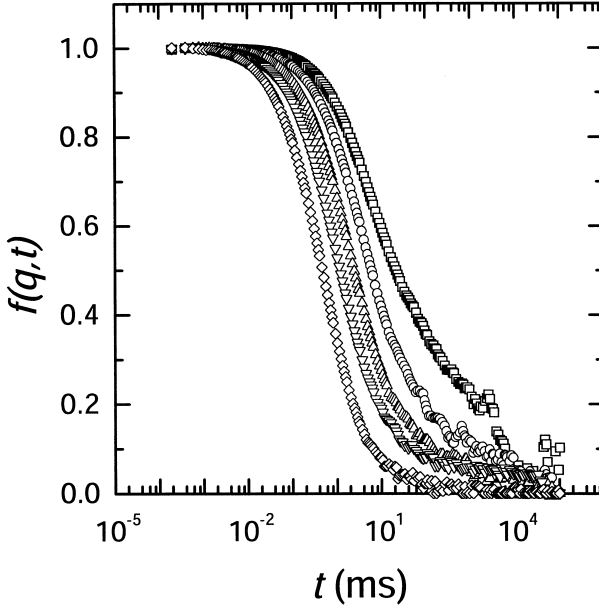


Fig. 1: Dynamic structure factor $f(q, t)$ for a “fine” fibrin gel (0.5 M NaCl) at concentration $c = 303$ nM and $q = 1.00, 1.14, 1.69, 2.40$, and $2.89 \times 10^5 \text{ cm}^{-1}$ (from left to right).

$$f(q, t) = 1 + \frac{\langle I(q) \rangle_T}{\langle I(q) \rangle_E} \left(\sqrt{g_T^{(2)}(q, t) - g_T^{(2)}(q, 0) + 1} - 1 \right) \quad (4)$$

where $\langle I(q) \rangle_T$ is the time-averaged scattered intensity detected during the measuring time T .

Experimental results

The dynamic structure factor of a “fine” fibrin gel grown in a solution 0.5 M NaCl, at fibrinogen concentration on $c = 303$ nM is reported in Fig. 1 versus the delay time t in lin-log plot. This gel is ergodic, so Eq. 3 and Eq. 4 can be equivalently used to obtain the dynamic

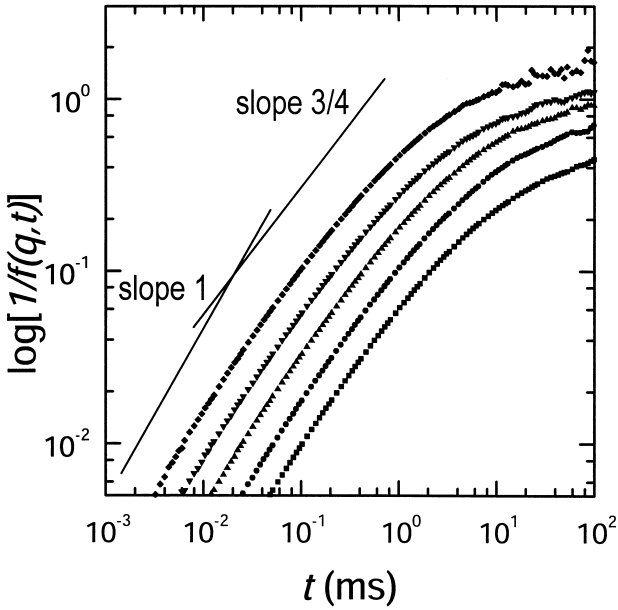


Fig. 2: Log-log plot of the $\log[1/f(q,t)]$ versus t for the same data of Fig. 1 ($q = 1.00, 1.14, 1.69, 2.40$, and $2.89 \times 10^5 \text{ cm}^{-1}$ from left to right). The dynamic structure factor change continuously from a mono-exponential decay at the shortest delay time to a stretched exponential decay as shown by the drawn lines of slope 1 (mono-exponential decay) and 3/4 (stretched exponential decay).

structure factor, and its dynamics appears to be fully developed for all the q values investigated, as evidenced by the fact that all the curves of Fig. 1 decay to zero. In order to analyze the asymptotic behaviour of the dynamic structure factor at the early delay times, the same data of Fig. 1 are reported in Fig. 2 as $\log[1/f(q,t)]$ as a function of t on a log-log plot. The solid lines have slope of 1 and of 3/4, respectively and the data taken at different q values were arbitrarily shifted for clarity. The curves show that, at the shortest times, $f(q,t)$ exhibits a mono-exponential (slope 1) relaxation, while at intermediate times $f(q,t)$ crosses over to a stretched exponential decay (slope 3/4) characterized by the exponent $\beta \sim 3/4$.

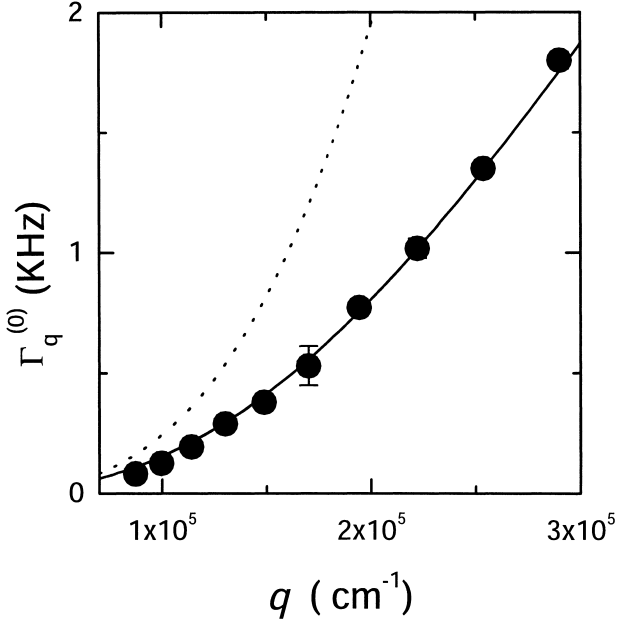


Fig. 3: The initial decay rate $\Gamma_q^{(0)}$ of the dynamic structure factor of the same sample of Figs. 1 and 2 is plotted against the wavevector q . The fit of Eq. 5 to the experimental data (full line) both with the theoretical prediction for Gaussian chains (dashed line) are also reported.

As recently reported³⁾ this behaviour, can be explained as due to the coupling of the long wavelength modes of single chain dynamics to the cooperative motion of the polymers ensemble²⁾. This holds for semiflexible polymer networks fulfilling the conditions^{2,10)} $a < q^{-1} < \xi < l_p, L$, where a is the average diameter of fibrin fibres, ξ the gel mesh size, l_p the persistence length and L the contour length. By assuming that the internal configurational dynamics dominates over the centre of mass and the rotational motions, and in the weakly bending rod limit, the dynamic structure factor, $f(q, t)$, is calculated to a good approximation with a stretched exponential at the intermediate times $f(q, t) \sim \exp -(\Gamma_q t)^{3/4}$, and as mono-exponential function $f(q, t) \propto \exp -(\Gamma_q^{(0)} t)$ for $t \rightarrow 0$, with a decay rate, $\Gamma_q^{(0)}$ given¹⁰⁾ by the equation

$$\Gamma_q^{(0)} = \frac{k_B T}{6\pi^2 \eta} q^3 \left[\frac{5}{6} - \log qa \right] \quad (5)$$

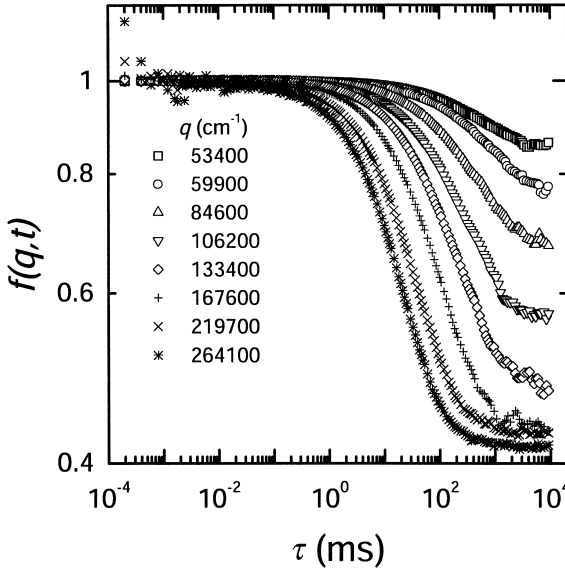


Fig. 4: Log-log plot of the dynamic structure factor $f(q,t)$ versus the decay time t for a “coarse” fibrin gel at 0.1 M NaCl salt concentration and at fibrin concentration $c = 330$ nM. The dynamics appears to be highly arrested with a plateau strongly dependent on q .

The average diameter a of semiflexible polymers forming the network thus can be obtained from the initial slope of $f(q,t)$, $\Gamma_q^{(0)}$, carried out by applying the cumulant method⁸⁾, and analysing its q dependence via Eq. 5, as shown in Fig. 3. The solid line (Eq. 5) fits well to the experimental data giving a value of $a=30\pm 5$ nm for the average diameter of the fibrin fibers. In the same figure, the clear deviation of the experimental data from the behaviour $\Gamma_q^{(0)} \sim q^3$, predicted for Gaussian²⁾ chains (dashed line), is also shown.

To investigate the effect of the fibers semiflexibility on the dynamics of the network structure we studied “coarse” gels which were obtained by decreasing the NaCl concentration of the gelling solution. These gels are highly non-ergodic, so Eq. 4 was used for obtaining the dynamic structure factor. To ensure a good statistics, the average scattered intensity

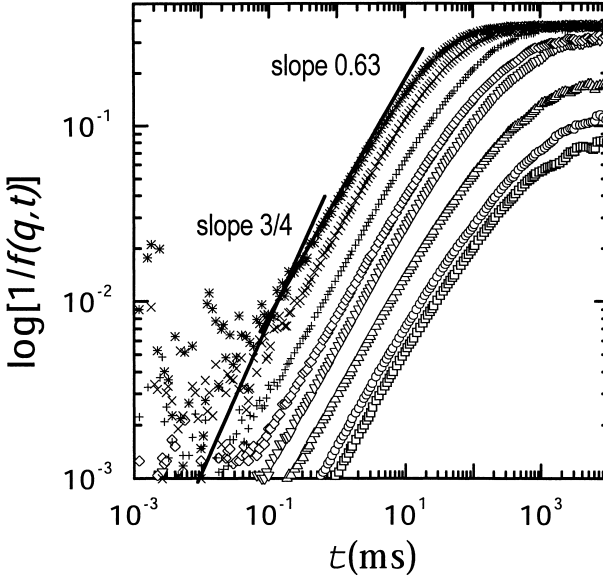


Fig. 5: Log-log plot of $\log[1/f(q,t)]$ versus delay time t for the same data of Fig. 4. The dynamics, both at the shortest and at intermediate delay times, exhibits a stretched exponential decay characterized by the exponent $\beta=0.63\pm0.07$, which is independent of q . For comparison, the exponent $\beta=3/4$ found for fine gels is also reported.

$\langle I(q) \rangle_E$ was measured at least on 10^5 different spatial configurations. Figure 4 reports a typical dynamic structure factor of a “coarse” gel for different q values. At the longest delay times the dynamics does not exhibit the expected relaxation, but it appears to be highly arrested, with $f(q,t)$ decaying to a plateau whose value strongly depends on q . At early times the dynamic structure factor $f(q,t)$ is characterized by a stretched exponential decay as shown by the slope the $\log[1/f(q,t)]$ plotted as a function of t in a log-log plot (Fig. 5). Ad variance with the behaviour observed for “fine” gels, the stretched exponential decay is observed even at the shortest delay times. Moreover, while both the plateau value and the decay time τ are q dependent, the exponent $\beta = 0.63\pm0.07$ is independent on q (Fig. 6).

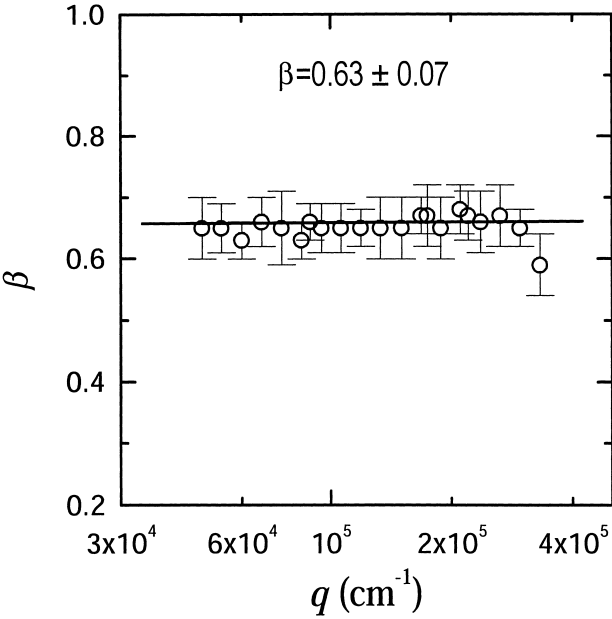


Fig. 6: Plot of the stretched exponent β versus the wavevector q . Solid line represent the mean value of $\beta = 0.63 \pm 0.07$.

Conclusions

The dynamics of semiflexible “fine” and “coarse” gels has been investigated by using DLS. “Fine” gels behave as typical semiflexible polymer gels, whose dynamic structure factor relaxes to zero showing an initial mono-exponential decay followed by a stretched exponential decay. From the mono-exponential decay it is possible to give an estimate of the average fibers diameter which turns out to be of the order of 30 nm. The dynamics behaviour of these gels has been interpreted as due to the coupling of the long wavelength modes of single chain dynamics to the cooperative motion of the polymers ensemble³⁾. On the contrary, “coarse” gels exhibit an highly arrested dynamics, whose dynamic structure factor decays to a plateau value q dependent. For these gels, the early time relaxation is characterized by a stretched exponential decay only, with an exponent $\beta = 0.63 \pm 0.07$ independently of q . The reported

results are remarkably similar to those recently observed on colloidal gels¹¹). According to the model proposed in Ref. 11, the internal dynamics of the gel can be interpreted as given by the contributions of the internal elastic modes of many different length scales. Moreover from the observed plateau, it is in principle possible to estimate the elastic modulus G of the gel. However when the theory developed in Ref. 11 is applied to polymer gels, the expected exponent should be $\beta=3/4$. The discrepancy between this value and the values measured for “coarse” gels is, to our knowledge, a controversial issue, that limits our understanding of the data.

In the attempt to shed some light on this problem, it should point out that, while the structure factor of the colloidal gel was measured at wavevectors *much smaller* than the reciprocal of the monomers diameter ($qa \ll 1$), for our “coarse” gels the measurements were taken at q vectors *comparable* with the reciprocal of the fibers diameter, being $a \sim 100\text{nm}$ ⁷⁾ and $q \sim 10^5\text{cm}^{-1}$, or larger. Thus we believe that, for applying the theory developed in Ref. 11 to our “coarse” gels, the contribution to the overall dynamics coming from the internal motion of the fibers, should also be taken into account. To investigate more deeply this problem, further measurements are currently in progress in our laboratory.

Acknowledgments

This work was supported by Ministero dell'Università e della Ricerca Scientifica e Tecnologica (MURST) and by Istituto Nazionale Fisica della Materia INFM.

References

1. *Polymer Gels*, D. DeRossi, K. Kajiwara, Y. Osada and A. Yamauchi (Eds.), Plenum Press, New York (1991)
2. K. Kroy, E. Frey in: *Scattering in Polymeric and Colloidal Systems*, W. Brown and K. Mortensen (Eds.), Gordon and Breach, (1999)
3. G. Arcovito, F. Andreasi Bassi, M. De Spirito, E. Di Stasio, M. Sabetta, *Biophys. Chem.* **67**, 287 (1997)

4. *Molecular Biology of Fibrinogen and Fibrin*, M. W. Mosesson and R. F. Doolittle (Eds.), Ann. NY Acad. Sci., New York (1983)
5. B. Blomback, *Thromb. Res.* **83**, 1 (1996)
6. J.W. Weisel, C. Nagaswami, L. Makosky, *Prot. Natl. Acad. Sci.* **84**, 8891 (1987)
7. M. De Spirito, G. Arcovito, F. Andreasi Bassi, M. Rocco, E. Paganini, M. Greco, F. Ferri, *Il Nuovo cimento* **20 D**, 627 (1998)
8. B. Berne, R. Pecora, *Dynamic Light Scattering*, Wiley, New York (1976)
9. P. Pusey, W. van Megen, *Physica* **157A**, 705 (1989)
10. K. Kroy, E. Frey, *Phys. Rev. E* **55**, 3092 (1996)
11. A.H. Krall, D.A. Weitz, *Phys. Rev. Lett.* **80**, 781 (1998)